



ChemComm

Facile light-initiated radical generation from 4-substituted pyridine under ambient conditions

Journal:	<i>ChemComm</i>
Manuscript ID	CC-COM-04-2020-002538.R1
Article Type:	Communication

SCHOLARONE™
Manuscripts

COMMUNICATION

Facile light-initiated radical generation from 4-substituted pyridine under ambient conditions

Received 00th January 20xx,
Accepted 00th January 20xx

• Ami Nakayama,^a Haru Kimata,^a Kazuhiro Marumoto,^{ab} Yohei Yamamoto^{ab} and Hiroshi Yamagishi^{*ab}

DOI: 10.1039/x0xx00000x

Photochemical reactions that generate stable radical species in ambient conditions find unique applications in the materials science. Here we present a facile photogeneration of a stable radical species from a 4-substituted pyridine derivative in the presence of water and air at room temperature. The radical generation reaction accompanies visible colour change into green and is repeatable for multiple times.

Photoinitiated radical generation reactions are pivotal chemical processes in the modern high-precision manufacturing.^{1–3} Radical species utilized for this purpose need to be reactive and therefore survive only temporarily.⁴ What if the photo-generated radical is sufficiently stable and unreactive to surrounding media? They may be no longer feasible in the organic synthesis but must be promising as photoswitchable chromic materials, imaging materials, and electroconducting materials.^{5–7} Actually, such photoresponsive radical generators are recently found to have unique applications in the field of materials science.^{8–10} Giuseppone and co-workers reported a photo-triggered radical generation of a triarylamine derivative.⁹ The radical generation leads to the self-assembly of the triarylamines into conducting one-dimensional fibres. Abe and co-workers developed a series of photochromic materials based on pentaarylbimidazole derivatives that afford biradical species spatiotemporally in response to the UV irradiation.¹⁰

Nonetheless, the library of such photoresponsive stable radical generators is still limited. This is in clear contrast with the field of persistent radical species, where tailored molecular designs have been established.^{5,6} For instance, the unpaired electron in α -nitronyl nitroxides are stable enough even in the non-deaerated conditions because the electron can delocalize around the oxygen and nitrogen atoms. The radical centre of

triphenylmethyl radicals is protected by sterically bulky substituents, leading to the kinetic stability. The difficulty in designing the photoresponsive stable radical generators is the lack of methodology for combining the photoresponsivity with the stability of the generated radical.

Radicals of pyridine derivatives are common intermediate species in organic chemical reactions. Minisci reaction, an alkylation reaction to heteroaromatic bases, proceeds through a radical cation intermediate.¹¹ Pyridine derivatives are also successful in the field of materials science. Radical cation forms of quaternized bipyridinium, viologens, are stable because of the reduced electron density in the aromatic rings as well as the delocalization among the two aromatic rings.^{12,13} Photoirradiation as well as chemical and electrochemical treatments can induce the formation of the radical form of viologen.¹⁴ By virtue of their vivid chromic behaviour and excellent tolerance toward electro- or chemical-redox processes, viologens have been utilized as a multi-functional building unit in the materials science.^{15,16} However, generation of analogous stable radical species from the synthetically more accessible analogue, neutral pyridine, still remains a



Fig. 1 (a) Schematic representations of the synthetic procedure for Py^{semi} from porous crystal Py^{open} and subsequent synthesis of pyridine radical in Py^{semi} by UV light irradiation. (b) Photographs of the powder samples of Py^{semi} put on a glass before (left) and after (right) the exposure to UV light (365 nm) for 1 min under non-deaerated conditions at 298 K.

^a Department of Materials Science, Faculty of Pure and Applied Sciences, University of Tsukuba, 1-1-1 Tennodai, Tsukuba, Ibaraki 305-8573, Japan. E-mail: yamagishi.hiroshi.ff@u.tsukuba.ac.jp

^b Tsukuba Research Centre for Energy Materials Science (TREMS), University of Tsukuba, 1-1-1 Tennodai, Tsukuba, Ibaraki 305-8573, Japan.

† Electronic Supplementary Information (ESI) available. See DOI: 10.1039/x0xx00000x

fundamental challenge, because pyridine has abundant electron density and less electron delocalization in the aromatic rings. Although several anion radicals of pyridine derivatives have recently been reported, they are still unstable in non-deaerated conditions.^{17,18}

Here we report a facile photoinitiated generation of stable radical species by using a porous molecular crystal made of a fully aromatic hexapyridyl compound **Py₆Mes** (Fig. 1a). The crystal was immersed into aqueous solution of an ammonium salt so that the water molecules can go inside the crystalline pore with the help of the added salt. The reaction was initiated by photoabsorption at the pyridyl rings and subsequently followed by the reaction with proximal water molecules. Half-life of the generated pyridine radical at room temperature was ~3.5 min, which is exceedingly longer than the typical pyridine radicals. Several ammonium and alkali salts also facilitate the analogous radical generation reactions. The radical generation reaction accompanied the coloration from transparent to green, demonstrating its usefulness for future chromic materials (Fig. 1b).

The host compound is a *D*_{3h}-symmetric, fully aromatic molecule **Py₆Mes** featuring three 3,5-bipyridylphenyl wedges that are connected to the central mesitylene core (Fig. 1a). We recently reported that **Py₆Mes** assembles, upon crystallization in acetonitrile (MeCN), into a nanoporous molecular crystal **Py^{open}** through multiple intermolecular C–H...N bonds (Fig. 1a).¹⁹ Even after the desolvation of the crystallization solvent MeCN, the porous framework of **Py^{open}** is unexpectedly stable against heating up to 475 K despite the lability of the C–H...N

bonds. We found that, based on the crystallographic study of its polymorphs, the polarity of the crystallization solvent affects the mode of the packing of **Py₆Mes**. Recrystallization from highly polar solvents such as MeCN or isopropanol yields porous crystals isostructural with **Py^{open}**, while non-porous inclusion crystals were obtained when moderately polar CHCl₃ or THF was employed instead of MeCN. We anticipated that highly polar solvent molecules tend to interact with the peripheral pyridyl rings of **Py₆Mes** via dipole–dipole attraction force. In fact, all the pyridyl rings of **Py₆Mes** are exposed to the pore surface so that they can envelope the included highly polar solvent molecules.

Based on this insight, we envisioned that water molecules, featuring relative permittivity as high as 80, may be captured into the micropores of **Py^{open}** via the dipole–dipole interactions with the pyridyl rings in a similar way of MeCN. However, the trial to incorporate the water molecules into **Py^{open}** was not successful. We immersed the crystalline powder of **Py^{open}** into 400 μL of water for 24 h. The powder was then collected up by filtration. Thermogravimetric analysis (TGA) exhibited a weight loss of 0.8 wt% when the powder was heated up to 473 K (Fig. S1), which was less than the value expected from the pore volume (3.5 wt%) of **Py^{open}**.¹⁹ In order to enhance the interaction between the pore surface and the water molecules, tetraethyl ammonium tetrafluoroborate (TEABF₄) was added as a surfactant. When the concentration of TEABF₄ increased to 1.1 M, **Py^{open}** efficiently adsorbed water molecules together with TEABF₄ into the pores. After incubation for 20 h at 298 K, the powder sample was collected by filtration and then dried under reduced pressure for 2 h. The amount of TEABF₄ incorporated in the crystal was 91 mol% of the **Py₆Mes** according to the ¹H NMR spectrum of the powder dissolved in D₂O solution of DCl (Fig. S2). Considering the weight ratio of **Py₆Mes** and TEABF₄, the water contents per **Py₆Mes** was 2.2 wt% (Fig. S1), which is more than doubled in comparison with the water uptake of pristine **Py^{open}**.

Py^{open} lost its crystallinity and became semicrystalline (**Py^{semi}**) after the immersion into the aqueous solution of TEABF₄. A powder X-ray diffraction (PXRD) pattern of the crystal after immersion to the TEABF₄ solution (Fig. S5, green line) exhibited loss of fine peaks that was observed before the immersion (Fig. S5, orange line). Fourier-transform infrared (FTIR) spectra of **Py^{semi}**, in comparison with **Py^{open}**, exhibited a band shift from 1497 to 1507 cm⁻¹ and a band enhancement at 1633 cm⁻¹, which are assignable to C=C and C=N stretching bands (Fig. S6). Except these two bands, the profile in the fingerprint region was kept virtually intact. The less crystallinity and vibrational mode change of **Py^{semi}** is attributed to the partial cleavage and swapping of the C–H...N bonds by the incorporated TEABF₄ and water molecules (Fig. 3b).

The electronic absorption spectra of an MeCN solution of **Py₆Mes** exhibited an absorption band below 320 nm (Fig. S7, orange curve). An analogous absorption band was also observed with the powder sample of **Py^{semi}**, although the band edge was redshifted to 450 nm (Fig. 2a, orange line) due to the molecular packing of **Py₆Mes**. Unexpectedly, upon irradiation with UV light (365 nm) for 1 min, the colour of **Py^{semi}** turned into

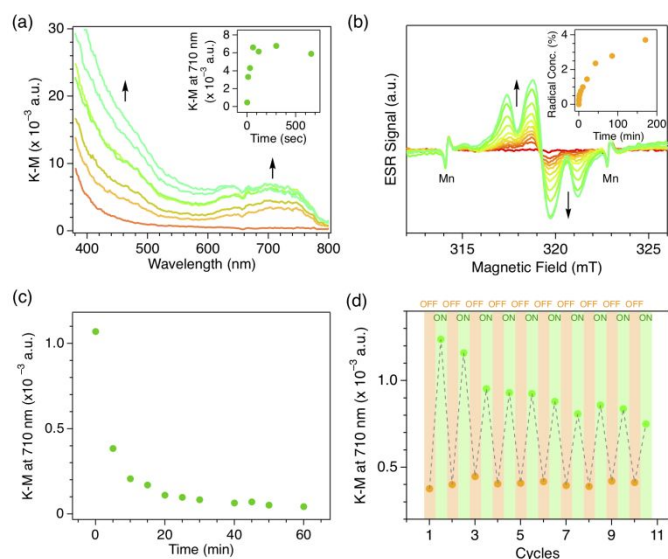


Fig. 2. (a, b) Diffuse reflectance spectra at 298 K (a) and ESR spectra at 20 K of **Py^{semi}** upon exposure to UV light. Insets show K-M values at 710 nm (a) and radical concentrations (b) of **Py^{semi}** plotted against the time of exposure to UV light. (c) A plot of K-M values of **Py^{semi}** against the incubation time at 298 K after the exposure to UV light for 3 min. (d) Changes in K-M value of at 710 nm **Py^{semi}** upon UV irradiation for 30 sec and subsequent incubation in dark for 1 h under non-deaerated conditions at 298 K.

green (Fig. 1b). Diffuse reflectance spectra of the powder sample of **Py^{semi}** exhibited, upon UV irradiation, a new absorption band centred at 710 nm, along with the enhancement of the shoulder peak below 500 nm (Fig. 2a). The spectral change at 710 nm saturates in 60 sec-irradiation with UV light (Fig. 2a inset).

This photochromic behaviour was observed only in the solid state containing TEABF₄. In fact, the electronic absorption spectra of MeCN solution containing **Py₆Mes** (100 μM) and TEABF₄ (100 μM) did not change even after the irradiation with UV light for 3 min (Fig. S7, green curve). Similarly, **Py^{open}** after immersion into deionized water instead of aqueous solution of TEABF₄ did not show any change in the diffuse reflectance spectra upon UV light irradiation (Fig. S8).

Photochromism is often a consequence of photochemical reactions such as photoisomerization reactions and photoinitiated radical generation reactions.^{8–10,20,21} To address this issue, we conducted electron spin resonance (ESR) measurements of **Py^{semi}** at 20 K with a quartz tube sealed with He gas. ESR spectrum of **Py^{semi}** before UV irradiation was featureless (Fig. 2b, red curve). A broadened triplet signal eventually emerged upon irradiation with UV light (Fig. 2b). The *g* value observed for **Py^{semi}** (2.00281) corresponds well with the reported *g* value of pyridinyl radical (2.00292).²² The triplet hyperfine structure indicates the interaction between the unpaired electron and the nitrogen atom in the pyridyl ring. The broadening of the hyperfine structure is attributed to the delocalization of the unpaired electron around the pyridyl and proximal phenyl rings.²³ Altogether, we attributed the origin of the photochromism to the generation of a radical species in the pyridyl rings of **Py₆Mes**. The radical concentration in **Py₆Mes** after UV light exposure for 85 min was as high as 2.8 % (Fig. 2b

inset). The radical concentration was not saturated even after further 170 min-irradiation (Fig. 2b inset).

The photogenerated radical in **Py^{semi}** survives for a certain minute even in the presence of water and air at 298 K. The K-M values at 710 nm plotted against the incubation time after the UV irradiation shows an exponential decay with half-life time of 3.5 min (Fig. 2c), which is extremely long in comparison with typical pyridine radicals that survive only a few seconds even under inert conditions.²⁴ The radical generation and quenching processes in **Py^{semi}** can be repeated at least 10 cycles. Fig. 2d shows the K-M values at 710 nm plotted as an indicator of the radical concentration in **Py^{semi}**. Each cycle consisted of the exposure of **Py^{semi}** to UV light for 30 s and subsequent incubation of **Py^{semi}** in dark for 1 h at 298 K. Even after the intense light exposure, the molecular structure of **Py₆Mes** was kept virtually intact as revealed by the ¹H NMR spectra (Figures S3 and S4).

Radical generation reaction from pyridyl rings was previously studied as a primal process in a photodegradation reaction of non-substituted pyridine in water (Fig. 3a).^{25,26} It is referred that, initially, pyridine absorbs UV light by the π–π* and n–π* transitions, yet the following process of the photodegradation is still unclear. We assume that the pyridine ring of **Py₆Mes** associates with a water molecule via hydrogen bond prior to the photoreaction. Subsequent photoabsorption most likely induces proton-coupled electron transfer between the excited pyridine and the water molecule, leading to the formation of a pyridine radical and a hydroxyl radical.

The photoreaction pathway of **Py^{semi}** was elaborated by using its dehydrated version. The dehydrated sample was prepared by annealing the powder sample of **Py^{semi}** at 423 K for 1 h under constant Ar flow. Even after irradiation with UV light

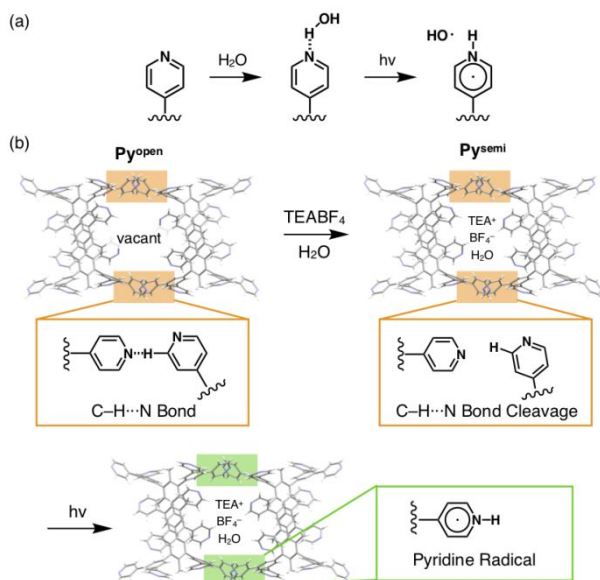


Fig. 3 (a) Proposed radical generation reaction in **Py^{semi}** upon irradiation with UV light in the presence of water. (b) Schematic representations for the C–H...N cleavage in **Py^{semi}** upon incorporation of water and TEABF₄ and subsequent radical generation reaction by UV irradiation to **Py^{semi}**.

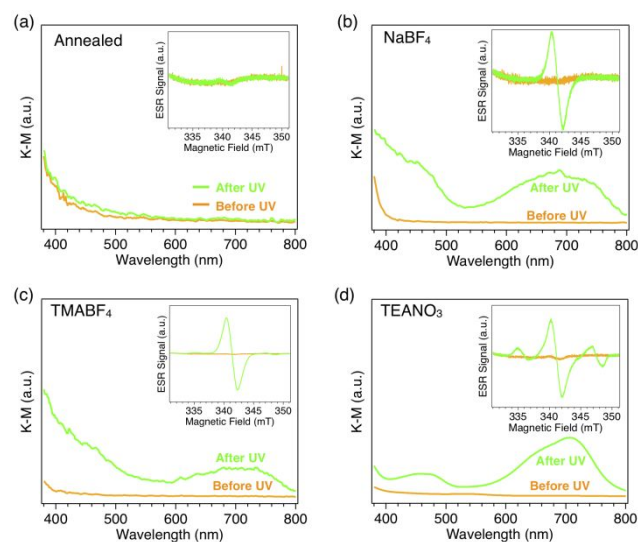


Fig. 4 Diffuse reflectance spectra **Py^{semi}** annealed at 423 K for 1.5 h (a), and **Py^{open}** immersed in aqueous solutions of NaBF₄ (b), TMABF₄ (c), and TEANO₃ (d) before (orange curves) and after (green curves) the exposure to UV light. Insets show ESR spectra of each sample measured before (orange curves) and after (green curves) the UV irradiation.

(365 nm) for 3 min, the annealed sample hardly showed photochromism (Fig. 4a) and ESR signal (Fig. 4a inset). This result corroborates the involvement of water molecules in the radical generation reaction.

A significant difference between the conventional photodegradation reaction and the reaction in **Py^{semi}** is the stability of the resultant radical species. The origin of the superior radical stability in **Py^{semi}** still remains uncertain, but we currently attributed to the electron delocalization and the suppressed thermal movement. The unpaired electron in **Py₆Mes** is energetically more stable than that in pyridine, because the unpaired electron on the pyridyl ring in **Py₆Mes** can delocalize around the phenyl ring substituted at the 4 position of the pyridyl ring. In addition, the sparse molecular packing in **Py^{semi}** due to the steric bulkiness of **Py₆Mes** and the restricted thermal motion may inhibit the radical recombination or hydrogen subtraction reactions with the neighbouring molecules and, thereby, prolong the lifetime of the radical species.

This radical generation reaction proceeds regardless of the chemical structure of the added salts. We utilized, instead of TEABF₄, aqueous solutions of tetraethylammonium nitrate (TEANO₃, 16 M), tetramethylammonium tetrafluoroborate (TMABF₄, 160 mM) and sodium tetrafluoroborate (NaBF₄, 8.9 M). The concentrations of the salts were not equivalent with each other due to their significantly different solubility in water. Crystalline powders of **Py^{open}** (5 mg) were immersed into 400 μL aqueous solutions of TEANO₃, TMABF₄, and NaBF₄, respectively, and then allowed to stand at 298 K. After the immersion for 20 h, the powders were collected by filtration and then dried under reduced pressure for 2 h.

According to the PXRD profiles, the crystallinity of the resultant powder samples was deteriorated in comparison with the pristine **Py^{open}** (Fig. S3). All the samples exhibited coloration into green upon UV irradiation. Their diffuse reflectance spectra exhibited new absorption bands at around 700–710 nm (Fig. 4a–d). ESR spectra after the UV irradiation exhibited prominent signals with *g* values in the range from 2.0035 to 2.0039 (Fig. 4b–d insets). Their hyperfine structures suggest delocalization of the unpaired electron among carbon atoms. The satellite ESR signals in Fig. 4d is likely due to the by-products from the photoreaction of the nitrate anion.^{27,28} These diffuse reflectance and ESR spectra consistently proved that the molecular structure of cations and anions do not play significant role in the radical generation reaction. Namely, the water molecules incorporated in the pores with the help of the ionic salt are crucial in the radical generation reaction.

In conclusion, we developed a facile light-initiated radical generation reaction with 4-substituted pyridyl rings by incorporating water and ionic salt into a porous molecular crystal. Resultant radical is stable in the presence of water and air at 298 K with a half-life time of 3.5 min. Colour change of the solid accompanied by the radical formation is beneficial for future sensing applications. The radical generation reactions proceed irrespective of the sort of the added cation and anion, demonstrating the potential versatility of this reaction toward diverse applications.

Conflicts of interest

There are no conflicts to declare.

Notes and references

- M. Chen, M. Zhong and J. A. Johnson, *Chem. Rev.*, 2016, **116**, 10167–10211.
- C. Mendes-Felipe, J. Oliveira, I. Etxebarria, J. L. Vilas-Vilela and S. Lanceros-Mendez, *Adv. Mater. Technol.*, 2019, **4**, 1800618.
- Y. Yagci, S. Jockusch and N. J. Turro, *Macromolecules*, 2010, **43**, 6245–6260.
- J. Hioe and H. Zipse, *Org. Biomol. Chem.*, 2010, **8**, 3609–3617.
- R. G. Hicks, *Org. Biomol. Chem.*, 2007, **5**, 1321–1338.
- I. Ratera and J. Veciana, *Chem. Soc. Rev.*, 2012, **41**, 303–349.
- S. van de Linde, I. Krstić, T. Prisner, S. Doose, M. Heilemann and M. Sauer, *Photochem. Photobiol. Sci.*, 2011, **10**, 499–506.
- A. J. Sindt, B. A. DeHaven, D. W. Goodlett, J. O. Hartel, P. J. Ayare, Y. Du, M. D. Smith, A. K. Mehta, A. M. Brugh, M. D. E. Forbes, C. R. Bowers, A. K. Vannucci and L. S. Shimizu, *J. Am. Chem. Soc.*, 2020, **142**, 502–511.
- E. Moulin, F. Niess, M. Maaloum, E. Buhler, I. Nyrkova and N. Giuseppone, *Angew. Chem. Int. Ed.*, 2010, **49**, 6974–6978.
- Y. Kishimoto and J. Abe, *J. Am. Chem. Soc.*, 2009, **131**, 4227–4229.
- F. Minisci, R. Bernardi, F. Bertini, R. Galli, M. Perchinummo, *Tetrahedron*, 1971, **27**, 3575–3579.
- L. Striepe and T. Baumgartner, *Chem. Eur. J.*, 2017, **23**, 16924–16940.
- J. Ding, C. Zheng, L. Wang, C. Lu, B. Zhang, Y. Chen, M. Li, G. Zhai and X. Zhuang, *J. Mater. Chem. A*, 2019, **7**, 23337–23360.
- W. Q. Kan, S. Z. Wen, Y. C. He and C. Y. Xu, *Inorg. Chem.*, 2017, **56**, 14926–14935.
- X. Y. Lv, M. S. Wang, C. Yang, G. E. Wang, S. H. Wang, R. G. Lin and G. C. Guo, *Inorg. Chem.*, 2012, **51**, 4015–4019.
- K. W. Shah, S. X. Wang, D. X. Y. Soo and J. Xu, *Polymers*, 2019, **11**, 1839.
- M. S. Denning, M. Irwin and J. M. Goicoechea, *Inorg. Chem.*, 2008, **47**, 6118–6120.
- J. Schröder, D. Himmel, D. Kratzert, V. Radtke, S. Richert, S. Weber and T. Böttcher, *Chem. Commun.*, 2019, **55**, 1322–1325.
- H. Yamagishi, H. Sato, A. Hori, Y. Sato, R. Matsuda, K. Kato and T. Aida, *Science*, 2018, **361**, 1242–1246.
- M. Irie, T. Fukaminato, K. Matsuda and S. Kobatake, *Chem. Rev.*, 2014, **114**, 12174–12277.
- H. M. D. Bandara and S. C. Burdette, *Chem. Soc. Rev.*, 2012, **41**, 1809–1825.
- R. W. Fessenden and P. Neta, *Chem. Phys. Lett.*, 1973, **18**, 14–17.
- Y. Wang, S. Rajca and A. Rajca, *J. Org. Chem.*, 2017, **82**, 7512–7518.
- S. Tero-Kubota, K. Akiyama, T. Ikoma and Y. Ikegami, *J. Phys. Chem.*, 1991, **95**, 766–770.
- Y. Zhang, L. Chang, N. Yan, Y. Tang, R. Liu and B. E. Rittmann, *Environ. Sci. Technol.*, 2014, **48**, 649–655.
- J. Jousot-Dubien and J. Houdard, *Tetrahedron Lett.*, 1967, **44**, 4389–4391.
- Y. A. Tsegaw, W. Sander and R. I. Kaiser, *J. Phys. Chem. A*, 2016, **120**, 1577–1587.
- S. Goldstein and J. Rabani, *J. Am. Chem. Soc.*, 2007, **129**, 10597–10601.